



# Boron Compound–Based Treatments Against Multidrug-Resistant Bacterial Infections in Lung Cancer In Vitro Model

Demet Celebi<sup>1,2</sup> · Ozgur Celebi<sup>3</sup> · Elif Aydin<sup>4</sup> · Sumeyye Baser<sup>3</sup> · Mustafa Can Güler<sup>5</sup> · Serkan Yildirim<sup>6</sup> · Ali Taghizadehghalehjoughi<sup>7</sup>

Received: 27 July 2023 / Accepted: 8 October 2023 / Published online: 26 October 2023  
© The Author(s), under exclusive licence to Springer Science+Business Media, LLC, part of Springer Nature 2023

## Abstract

Multidrug-resistant bacteria is one of the most important public health problems. Increasing rates of antibacterial resistance also affect the outcomes of medical approaches. Cancer treatment because of immune system deficiency (chemotherapy or steroids usage) commonly can cause infection. Lung cancer is the dominant cause of cancer-related deaths, and infection is the most common cause of death among those patients. In this study, it was aimed to determine the antimicrobial, antibiofilm, and anticancer activity of boron compounds. A549 lung cancer cell line was infected with *Acinetobacter baumannii* (ATCC 19606), *Klebsiella pneumoniae* (ATCC 700603), and *Pseudomonas aeruginosa* (ATCC 27853). In order to determine the fractional inhibitory concentration (FIC) index, antibiotics and boron compound concentrations prepared according to the minimum inhibitory concentration (MIC) values were determined by the checkerboard method. In our study results, the antibiofilm activity was an average of 46% in *A. baumannii*+boron compounds, 45% in *P. aeruginosa*+boron compounds, and 43% in *K. pneumoniae*. Cell culture analysis results show a decrease in viability and antioxidant capacity and an increase in total oxidant status after adding boron compounds to the culture. Immunofluorescence results show a correlation with MTT, and boron compounds increased 8-OHdG expression in comparison to antibiotic administration. In conclusion, boron compounds have promising effects on bacteria, especially in resistant bacteria spp.

**Keywords** Antibacterial activity · Boron compounds · Drug resistance lung cancer · Sodium perborate monohydrate · Zinc borate · Etidote

## Introduction

Infections are frequent in patients who suffer from cancer. Antibiotic failure in patients with cancers will increase the frequency of sepsis, sepsis-related mortality, and sepsis-associated prices of care. In addition, chemotherapy, surgery, and radiation used for treatment cause opportunistic infections and death associated with this infection [1–3]. The rapid spread of antibiotic resistance can be seen in *P. aeruginosa*, *K. pneumoniae*, and *A. baumannii* bacteria [4].

Bactericidal and broad-spectrum antibiotics with  $\beta$ -lactam structure are carbapenems. Infections brought on by gram-positive and gram-negative bacteria are treated with them [5, 6]. Initially, only life-threatening illnesses were treated with carbapenems alone [7, 8]. Gr (–) lines that are resistant to carbapenem have emerged as a result of widespread use [9]. Carbapenemases are categorized based on Ambler class A (KPC, IMI, PER, SME, GES, etc.), class D (OXA-23 and OXA 48), and class B (NDM,

✉ Demet Celebi  
celebiidil@atauni.edu.tr

<sup>1</sup> Department of Microbiology, Faculty of Veterinary Medicine, Ataturk University, 25240 Erzurum, Turkey

<sup>2</sup> Ataturk University Vaccine Application and Development Center, Ataturk University, 25240 Erzurum, Turkey

<sup>3</sup> Department of Medical Microbiology, Faculty of Medicine, Ataturk University, 25240 Erzurum, Turkey

<sup>4</sup> Vocational School of Health Services, Kütahya Health Sciences University, Kütahya, Turkey

<sup>5</sup> Department of Medical Physiology, Faculty of Medicine, Atatürk University, Erzurum, Turkey

<sup>6</sup> Department of Pathology, Faculty of Veterinary Medicine, Ataturk University, 25240 Erzurum, Turkey

<sup>7</sup> Department of Medical Pharmacology, Faculty of Medicine, Seyh Edebali University, 11000 Bilecik, Turkey

GIM, VIM, IMP, SIM, AIM) enzymes. Class B enzymes are also called metallo  $\beta$ -lactamases [10].

Biofilms are extraordinarily virulent structures that can form communities and talk to each other. A matrix of polysaccharide matrix plates surrounds the biofilms, allowing them to adhere to all living and non-living surfaces [11]. It has been decided that microorganisms with a biofilm shape have one thousand instances greater resistant to antibiotics than planktonic types [12]. The biofilm type causes difficulties in the treatment of infections and leads to the use of multiple antibiotics [13]. It is known that *P. aeruginosa*, *K. pneumoniae*, and *A. baumannii* pathways that use screening cells as a result of suppression of the immune system in cancer patients lead to prognosis cells. Even in non-cancerous pneumonia groups, these microbes exhibit severe clinical pictures. Fighting these bacteria in cancer patients poses a much bigger problem. Increasing antimicrobial resistance and the inadequacy of existing preservatives are triggering the search for antimicrobials. In this context, boron receptors were found to be of interest in this area of study due to their anti-effective, anti-carcinogenic, antiviral, and anti-inflammatory residues. One of the special factors that has organic consequences on living things is boron [14]. Boron has been confirmed to be essential in the life cycles [15–17]. According to recent studies, it is important to look into the protein-biomolecular interactions, anticancer, antibacterial, drug delivery, and organic characteristics of boron compounds. In our study, boron compounds (SPM sodium perborate monohydrate, ZB zinc borate, Etidote disodium octaborate tetrahydrate) were used for treating the A549 lung cancer model infected with *A. baumannii*, *K. pneumoniae*, and *P. aeruginosa*. We try to determine the boron compounds' antimicrobial, antibiofilm, and anticancer activity in an in vitro model.

## Material and Method

### Chemical and Reagent

3-(4,5-Dimethylthiazol-2-yl)-2,5-diphenyltetrazolium bromide (MTT, fetal bovine serum (FBS), SPM, ZB, and Etidote), antibiotic antimetabolic solution, dimethyl sulfoxide (DMSO), Muller-Hinton (MH) medium, Luria-Bertani (LB), plate count agar (PCA), and trypsin-EDTA were obtained from Sigma-Aldrich (St. Louis, MO, USA). Total antioxidant capacity (TAC) and total oxidant status (TOS) were obtained from Rel Assay Diagnostics, Turkey. Taq polymerase and SYBR safe DNA gel stain were obtained from Sigma-Aldrich (St. Louis, MO, USA).

### Preparation of Boron Compounds

Commercially available SPM, ZB, and Etidote (Sigma-Aldrich) compounds were prepared mechanically in DMSO (5 mg/ml) and the medium [18, 19].

### Bacteria Strain

*A. baumannii*, *P. aeruginosa*, and *K. pneumoniae* strains were used. One hundred microliters of Luria-Bertani (LB) was added to the bacterial stock and incubated at 37 °C for  $18 \pm 24$  h at 150 rpm. Then, it was inoculated into a fresh LB medium.

### Determination of MIC and FIC Values

The antibacterial exertion of boron-deduced composites SPM, ZB, and Etidote was tested using the broth microdilution system. In this study, *A. baumannii* (ATCC19606), *P. aeruginosa* (ATCC 27853), and *K. pneumoniae* (ATCC 700603) bacterial strains were used. In the study, the Clinical and Laboratory Norms Institute (CLSI) standardized system was performed with some variations. Compactly, the bacteria were cultivated in Muller-Hinton (MH) medium for 24 h after being subcultured overnight on Luria-Bertani (LB) agar plates. In 96-well plates, after dispensing MH medium (100  $\mu$ l), meropenem, piperacillin-tazobactam, ampicillin-sulbactam (Sigma-Aldrich, USA; 128  $\mu$ l/ml), and sodium perborate tetrahydrate (SPM), zinc borate (ZB), and Etidote composites (5 mg/ml) were used as reference. Suspicious results of 100  $\mu$ l of boron composites in MH medium were sequentially decocted starting at 1024  $\mu$ g/ $\mu$ l. A 0.5 McFarland-adjusted bacterial suspension (100  $\mu$ l) was dispensed. The plate was incubated at 37 °C for 24 h. The growth window of the bacteria was covered with optic viscosity at 600 nm (OD600), and ELISA anthology multimode microplate compendiums (BioTek ELX800; BioTek Instruments, Inc.) were measured every 20 min. MICs were used to determine the lowest concentration of antimicrobial agents that prevent the conspicuous growth of bacteria [18–20].

### Quantitative Estimation of Biofilm Formation in *A. baumannii* (ATCC19606), *P. aeruginosa* (ATCC27853), and *K. pneumoniae* (ATCC700603) Isolates

Bacterial strains were anatomized for their ability to form biofilms using the crystal violet test. The bacterial viscosity was acclimated to the McFarland standard of 0.5. The bacteria were plated in triplicate in 200- $\mu$ l 96 concave plates and incubated at 37 °C for 24 h. The plate was reversed, and the conjoined cells were washed with phosphate-buffered

saline (1X PBS, pH 7.4) three times. Demitasse violet 200  $\mu\text{l}$  0.1 w/v was used to dye the biofilm biomass for 20 min at room temperature. The demitasse was thrown into the vial, and excess stains were washed off the plates doubly with 1X PBS. Thermo Scientific Multiskan GO was used to measure the OD at 570 nm and further dissolve the color that the adhering cells had retained in 200  $\mu\text{l}$  95 ethanol by incubating for 20 min. To evaluate the level of biofilm conformation, OD570 was utilized. The isolates were indicated as “high biofilm formers (HBF)” or “low biofilm formers (LBF)” using predefined criteria [18–20].

### Combination Application of *A. baumannii* (ATCC19606), *P. aeruginosa* (ATCC27853), and *K. pneumoniae* (ATCC700603) with Boron Compounds

The best MIC for boron composites was created by combining several components. The bacterial strains were drained from the plates in an examination that followed a similar procedure to the biofilm evaluation test concept after 48 h. Each well then received 200  $\mu\text{l}$  of glucose-fortified culture media with TTC (5 mg/ml) before being cultured for 3 to 4 h at 37 °C. The intensity of the red color was measured at 570 nm at the conclusion of the test, at which point it was recognized as a measure of the quantity of living cells. The outcomes of the controls were compared [18, 19].

### Checkerboard Method

Clinical and Laboratory Standards Institute (CLSI) and European Committee for Antimicrobial Vulnerability Testing (EUCAST) standards state that when the in vitro efficacy of antibiotic combinations is performed, the effect is attained effectively if it is advanced than the total effect attained when the same medicines are used alone, synergistic commerce is achieved if the addition is equal, and cumulative commerce is attained as a result of both test results being inversely lower [19].

### Fractional Inhibitory Concentration (FIC) Index Calculation

It was used in accordance with the FIC index formula, which was used to assess how well the combinations worked. The algorithm  $< 0.5$  indicates synergy,  $0.5\text{--}1$  indifference, and  $> 1$  antagonism was used to determine the outcomes [19].

### Resistance Modeling

Resistance modeling is used to determine the possible development of resistance in isolates exposed to an antimicrobial agent. Antibiotic resistance development methods in bacteria in vitro have been studied in two ways: single or multi-stage.

### Single-Stage Resistance Modeling

It is a method to determine the resistance of isolates exposed to the inhibitory concentrations of antimicrobial agents. For this purpose, 100  $\mu\text{l}$  of  $\sim 10^9\text{--}10^{10}$  CFU/ml bacteria was inoculated with PCA medium containing synthesized SPM, ZB, and Etidote compounds (according to MIC). After 96 h of incubation, isolates that formed colonies were considered resistant [21].

### Multi-stage Resistance Modeling

The serial passaging technique, which is a standard method in multi-stage resistance modeling, was used. In this method, isolates exposed to antimicrobial agents were continuously subcultured, and their resistance was studied; first, 100  $\mu\text{l}$  of  $\sim 10^9\text{--}10^{10}$  CFU/ml bacteria was inoculated in a PCA medium containing MIC concentrations of SPM, ZB, and Etidote compounds. The MIC values of the isolates were determined again by taking the colonies growing in the medium, and resistance formation was evaluated according to the isolates with changes in MIC values. The test was terminated in the passage where no colonies were observed in the media [22].

### Molecular Analysis

#### DNA Isolation

The birth of total DNA from bacterial lines was carried out by way of a boiling system. The microorganism has been planted in a 3 ml LB medium and grown for 20 h at 37 °C in a shaker incubator. The 1.5 ml subculture was once placed in a microcentrifuge tube. After precipitation at 13,000 rpm for 1 ns, the supernatant was discarded, and the lead was dissolved in 1 ml deionized water by vortexing. This washing process was repeated three times. Additionally, the cells were broken down by heating at 100 °C for 10–15 min. The residue was collected with the aid of centrifugation at 4 °C at 13,000 rpm for 10 min. The supernatant was transferred into a smooth microcentrifuge tube and saved in a deep freezer for use in PCR [23].

#### Detection of Carbapenemase Genes

Multiplex PCR was used to analyze the broad-spectrum beta-lactamase resistance genes. OXA-48 was employed in this system together with PCR factors and related AIM instructions (Table 1) [24]. The response was performed in 25  $\mu\text{L}$  volume and 2.5-  $\mu\text{L}$  PCR buffer (10X), 0.5-  $\mu\text{L}$  dNTP admixture (10 mm), 10 pmol 0.5-  $\mu\text{L}$  F and 0.5-  $\mu\text{L}$  R primers. It was formed from 0.2  $\mu\text{L}$  Taq polymerase (Thermo Scientific, MO, USA), 1.5  $\mu\text{L}$  (25 mM)  $\text{MgCl}_2$ , 18.3  $\mu\text{L}$

**Table 1** Amplicon sizes and references were employed with oligonucleotide primer sequences [22]

Primer name	Primer sequence (5'–3')	Gene	Product size (bp)
OXA-F	GCGTGGTTAAGGATGAAC AC	<i>bla</i> <sub>OXA-48</sub>	438
OXA-R	CATCAAGTTCAACCAACCG		
AIM-F	CTGAAGGTGTACGGAAAC AC	<i>bla</i> <sub>AIM</sub>	322
AIM-R	GTTCGGCCACCTCGAATTG		

H<sub>2</sub>O, and 1 µl DNA template. The modification was performed under thermal cycle conditions [25]. DNA fractions visualized by gel electrophoresis in 1.5 agarose gel at 100 V for 1 h at 1X TAE containing SYBR Safe DNA gel stain (Thermo Scientific, MO, USA) (40 mmol/l Tris-HCl (pH 8.3), 2 mmol/l acetate, 1 mmol/l EDTA) and imaged by UV light. The performing videotapes were compared with a 100 bp plus DNA Ladder.

### A549 Lung Cancer Cell Line Preparation

A549 human lung cancer cell line (ATCC no: CCL-185) was used for the study. Frozen cells were rapidly thawed, and cells were seeded in a 25-cm<sup>2</sup> flask (DMEM high glucose, 10% FBS, and 1% antibiotics (penicillin, streptomycin, and amphotericin B)). Cells were collected and transferred to 96-well cell culture plates using trypsin-ethylenediamine-tetraacetic acid ((EDTA) 0.25% trypsin, 0.02% EDTA) once 80% of the flasks were covered with cells (10<sup>4</sup> cells/well).

### Preparation of Bacteria and Boron Components

SPM, ZB, Etidote compounds, *A. baumannii* (ATCC19606), *K. pneumoniae* (ATCC700603), and *P. aeruginosa* (ATCC27853) were used in the present study.

Groups ( $n = 10$ ):

1. Control group: the group containing only medium
2. Positive control group: DMSO (dimethyl sulfoxide) was used
3. Bacterial and antibiotic control group: *Pseudomonas aeruginosa* (10<sup>8</sup> CFU/ml) and piperacillin-tazobactam
4. Bacterial and antibiotic control group: *Acinetobacter baumannii* (10<sup>8</sup> CFU/ml) and meropenem
5. Bacterial and antibiotic control group: *Klebsiella pneumoniae* (10<sup>8</sup> CFU/ml) and ampicillin-sulbactam
6. Dose (µg/ml): Etidote+SPM (125 µl/ml) + (62.5 µl/ml)
7. Dose (µg/ml): SPM+ZB (62.5 µl/ml) + (31.25 µl/ml)
8. Dose (µg/ml): ZB+Etidote (31.25 µl/ml) + (125 µl/ml)

### MTT Analysis (Cytotoxicity Analysis)

The MTT analysis was done according to the manufacturer's procedure. Then, 10 µl of MTT solution was added and incubated at 37 °C for 4 h with 5% CO<sub>2</sub>. At the end of the time, the formazan crystals formed were dissolved by adding dimethyl sulfoxide (DMSO) solution (100 µl). Cell viability (%) was measured at 570 nm using a Multiskan GO microplate spectrophotometer. The viability rates of DMSO, bacteria, and antibiotics were compared with the control group. The treatment viability ratio was compared to the bacteria control groups. The percentage viability of the cells was calculated as follows:

$$\% \text{viability: (sample OD/control OD)} \times 100$$

### Oxidative Stress (TAC and TOS Assays) Analysis

Total antioxidant capacity (TAC) and total oxidant levels (TOS) were measured with a commercial kit (Rel Assay Diagnostics) according to the manufacturer's instructions. TAC (660 nm) and TOS levels (530 nm) were measured using a Multiskan GO microplate spectrophotometer (Thermo Fisher Scientific, Inc.).

### Immunofluorescence

For 30 min, the cells were treated in a paraformaldehyde solution. After that, the cells were exposed to 3% H<sub>2</sub>O<sub>2</sub> for 5 min. A total of 0.1% Triton-X solution was drip-applied to PBS-washed cells. It was made to wait for 15 min. At the end of the incubation period, the protein blocks were dropped and left in the dark for 5 min. After that, the primary antibody (8-OHdG cat no. sc-66036, dilution ratio: 1/100 USA) was applied and incubated in accordance with the provided instructions. As a secondary marker, an immunofluorescent secondary antibody (FITC floor no.: ab6785) was employed (diluent ratio: 1/500, UK) for 45 min while being kept in the dark. DAPI was then dripped onto the sections together with the filler (floor no.: D1306; dilution ratio: 1/200 UK) and left in the dark for 5 min, and the sections were closed with a lamella. A fluorescent microscope (Zeiss AXIO Germany) was used to look at the stained sections [19].

### Statistical Analysis

Five arbitrary locations from each image were selected in order to evaluate the amount of positive staining from the biofilm that had been achieved as a result of the dyeing. This was done using the ZEISS Zen Imaging Software. Statistics were used to characterize the data as mean and standard deviation (mean SD) for the stained areas. To compare immunopositive stained areas and immunoreactive cells with unharmed controls, one-way ANOVA and Tukey's tests were run. The test's results indicated that a value of  $P < 0.05$  was significant, the data were

**Table 2** Boron compounds used in the study

Name	Brand	Linear formula	Molecular weight	Cas number	Synonym	40 mM stock solution	1 l/medium
SPM	Sigma-Aldrich	BNaO <sub>3</sub> .H <sub>2</sub> O	99.81	<u>231-556-4</u>	*	99.815	3.993
ZB	Sigma-Aldrich	Zn <sub>3</sub> BO <sub>6</sub>	313.754	<u>10361-94-1</u>	Boric acid, zinc salt	313.754	12.550
Etidote	Eti Maden	Na <sub>2</sub> BO <sub>13</sub> .4H <sub>2</sub> O	412.527	<u>12280-03-4</u>	*	412.53	16.501

SPM sodium perborate monohydrate, ZB zinc borate, Etidote disodium octaborate tetrahydrate

**Table 3** Antimicrobial susceptibility

Bacterial strain/MIC (µg/l)	Meropenem	SPM	Etidote	ZB
<i>A. baumannii</i> (ATCC19606)	2	128	256	512
Bacterial strain/MIC (µg/l)	Piperacillin-tazobactam	SPM	Etidote	ZB
<i>P. aeruginosa</i> (ATCC27853)	16	256	256	256
Bacterial strain/MIC (µg/l)	Ampicillin-sulbactam	SPM	Etidote	ZB
<i>K. pneumoniae</i> (ATCC700603)	> 64	256	128	128

SPM sodium perborate tetrahydrate, ZB zinc borate

then presented as mean (±) standard error (S.E.), and a DNA Ladder of at least 100 bp was compared.

## Results

Boron compounds used in the study were prepared from a stock solution of 40 mM, 1024 µg/l. Necessary information about boron compounds is given in Table 2.

## MIC and FIC Values

In our study, minimal inhibition concentrations of antibiotics and boron compounds were determined against bacterial strains. The MIC concentration of antibiotics and boron compounds against bacterial strains is shown in Table 3.

To calculate the FIC index, antibiotic and boron compound concentrations created in accordance with MIC

**Table 4** Fractional inhibitory concentration index on *A. baumannii* (ATCC19606), *P. aeruginosa* (ATCC27853), *K. pneumoniae* (ATCC 700603), Etidote+SPM, Etidote+ZB, and ZB+SPM

Boron compounds/bacterial strain	<i>A. baumannii</i> (ATCC19606) (µg/ml)	<i>P. aeruginosa</i> (ATCC27853) (µg/ml)	<i>K. pneumoniae</i> (ATCC700603) (µg/ml)
Etidote+SPM	64 + 1024 (S) 128 + 512 (S) (512 – 128) + 1024 (Ad) Other doses are ineffective	(128 – 32) + 32 (S) (64 – 32) + 1024 (Ad) (512 – 128) + 64 (Ad) (512 – 256) + 32 (Ad) Other doses are ineffective	64 + 32 (S) 64 + 512 (S) 32 + 64 (S) (64 – 32) + 32 (S) (512 – 128) + 1024 (Ad) 128 + 512 (Ad) 32 + 512 (Ad) 1024 + 64 (Ad) Other doses are ineffective
Etidote+ZB	256 + 1024 (Ad) 128 + 512 (Ad) Other doses are ineffective	(64 – 32) + 64 (S) 32 + 256 (Ad) 512 + 128 (Ad) 32 + 128 (Ad) Other doses are ineffective	(64 – 32) + 64 (S) (64 – 32) + 32 (S) 128 + 64 (Ad) Other doses are ineffective
ZB+SPM	256 + 1024 (Ad) 128 + 512 (Ad) Other doses are ineffective	32 + 32 (S) (64 – 32) + 1024 (Ad) (64 – 32) + 64 (Ad) 64 + 32 (Ad) Other doses are ineffective	(128 – 64) + 32(S) 32 + 256 (Ad) 32 + 128 (Ad) (64 – 32) + 64 (Ad) 256 + 32 (Ad) 32 + 32 (Ad) Other doses are ineffective

**Table 5** Antibiofilm activity in boron compounds

Bacteria strains ATCC no+boron compounds	Positive control	Negative control	Highest OD value
<i>A. baumannii</i> (ATCC19606)			3.270
<i>A. baumannii</i> (ATCC19606)+Etidote+SPM	0.795	0.119	1.750
<i>A. baumannii</i> (ATCC19606)+Etidote+ZB			1.700
<i>A. baumannii</i> (ATCC19606)+ZB+SPM			1.820
<i>P. aeruginosa</i> (ATCC27853)			2.850
<i>P. aeruginosa</i> (ATCC27853)+Etidote+SPM	0.795	0.317	1.690
<i>P. aeruginosa</i> (ATCC27853)+Etidote+ZB			1.433
<i>P. aeruginosa</i> (ATCC27853)+ZB+SPM			1.481
<i>K. pneumoniae</i> (ATCC700603)			2.990
<i>K. pneumoniae</i> (ATCC700603)+Etidote+SPM	0.795	0.305	1.793
<i>K. pneumoniae</i> (ATCC700603)+Etidote+ZB			1.644
<i>K. pneumoniae</i> (ATCC700603)+ZB+SPM			1.661

values were examined based on the FIC index calculation. All these values are shown in Table 4.

## Biofilm Results

At a wavelength of 570 nm, antibiofilm activity against biofilm capacity was tested. Table 5 provides a summary of the findings. According to the findings, the structure of the

boron compound reduced the growth of biofilm. According to the findings of our study, the antibiofilm activity of *A. baumannii* (ATCC19606)+boron compounds was found to be 46.48%, 48.01%, and 44.34%; that of *P. aeruginosa* (ATCC27853)+boron compounds to be 40.70%, 49.71%, and 48.03%; and that of *K. pneumoniae* (ATCC 700603) to be 40.03%, 45.01%, and 44%.

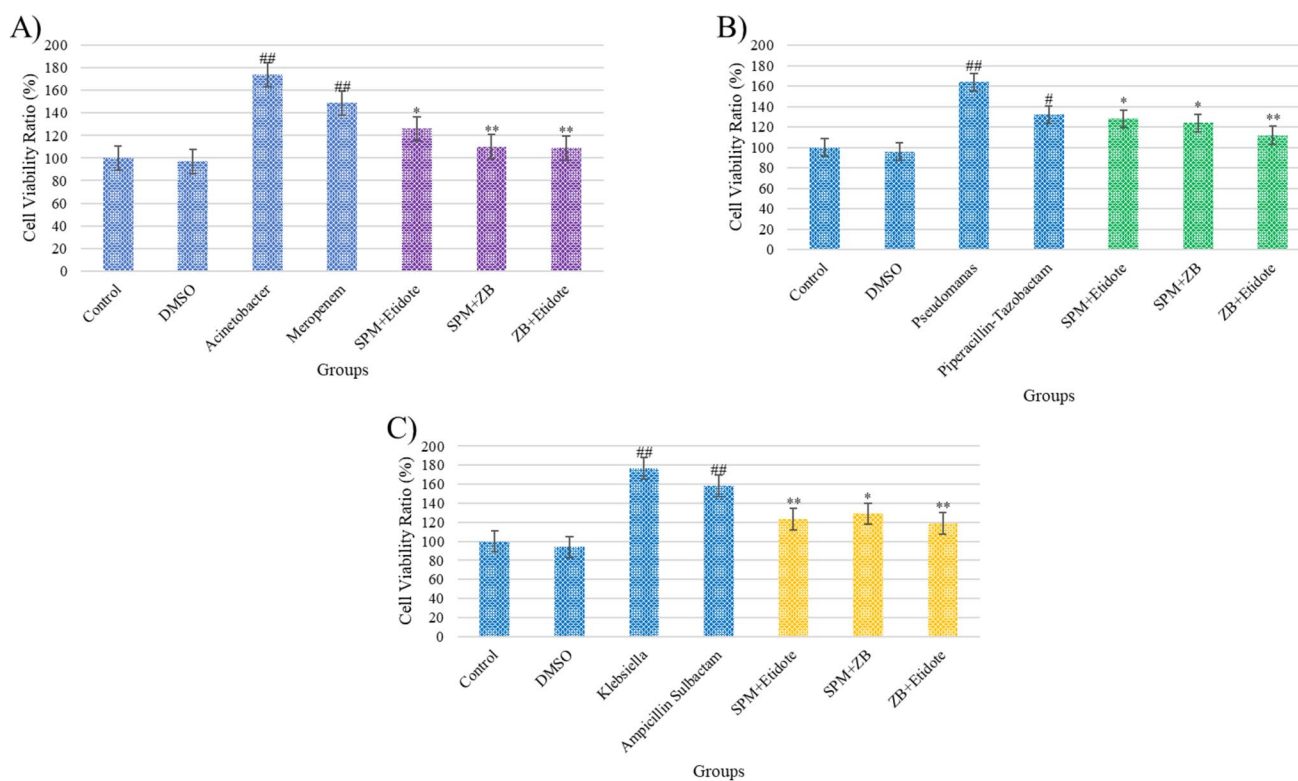


**Fig. 1** MTT (cytotoxicity) assay test. MTT assay results for **A** Acinetobacter—A549, **B** Pseudomonas aeruginosa—A549, and **C** Klebsiella pneumoniae—A549, in cell culture after 24 h. # $P < 0.05$  and

## $P < 0.001$  compared with the control group. \* $P < 0.05$  and \*\* $P < 0.001$  compared with the bacteria control group

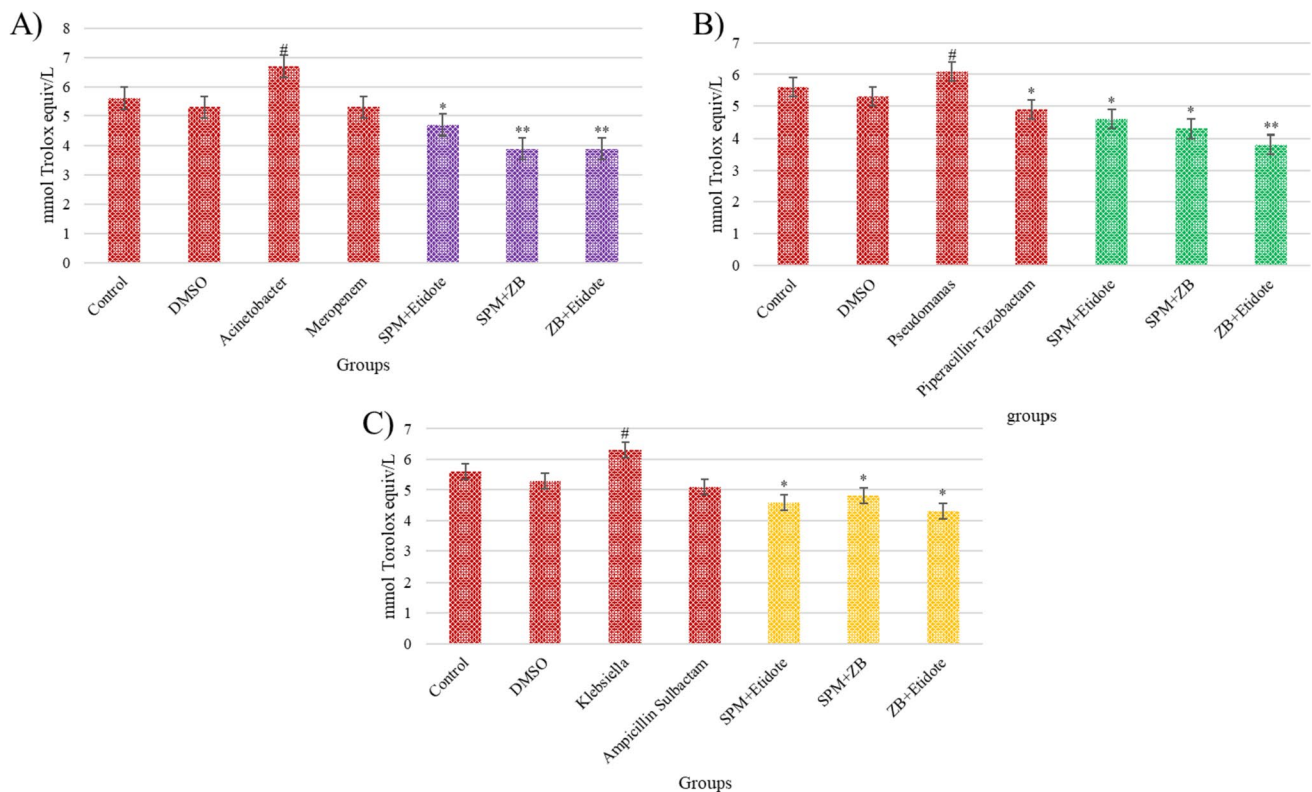


**Fig. 2** TAC (total antioxidant capacity) assay test. TAC assay results for **A** *Acinetobacter*—A549, **B** *P. aeruginosa*—A549, and **C** *K. pneumoniae*—A549, in cell culture after 24 h. # $P < 0.05$  compared with

the control group. \* $P < 0.05$  and \*\* $P < 0.001$  compared with the bacteria control group

## Resistance Modeling Results

In vitro resistance development studies were carried out on the possible resistance of the isolates against the synthesized compounds. In single-stage resistance studies conducted for this purpose, the detection of resistant isolates exposed to antimicrobial agents, in multi-stage resistance studies, it was aimed to observe the formation of resistant isolates over time as a result of exposing bacteria to antimicrobial agents in many passages.

### Single-Stage Resistance Modeling

Antibacterial agents (SPM, ZB, and Etidote) and positive controls (piperacillin-tazobactam for *P. aeruginosa*, meropenem for *A. baumannii*, and ampicillin-sulbactam for *K. pneumoniae*) were used against *A. baumannii* (ATCC19606), *K. pneumoniae* (ATCC700603), and *P. aeruginosa* (ATCC27853) isolate. It was applied at the same concentrations as the MIC. Among the compounds synthesized and found to be antibacterial by the MIC method, SPM was 256  $\mu\text{g/l}$  in all bacteria, ZB was 512  $\mu\text{g/l}$  in *A. baumannii* strain and 256  $\mu\text{g/l}$  in others, Etidote was 256  $\mu\text{g/l}$  in all

strains, and no bacterial growth was observed, while growth was observed in all negative controls containing DMSO.

### Multi-stage Resistance Modeling

In multi-stage resistance modeling, isolates were inoculated separately into the medium containing the MIC concentrations of the synthesized SPM, ZB, and Etidote compounds, and MIC values were redetermined. A lower concentration of the MIC value as a result of the application was determined, and the passaging process was continued until no growth was observed. The test was terminated when bacterial growth was not observed. No difference was detected in all isolates in the re-calculation of the MIC value. From the results of resistance modeling studies, it was observed that the isolates did not develop resistance in vitro.

## Cell Culture Analysis

### MTT Results

The present study then examined how the boron compound affects the viability ratio of bacteria combined with A549

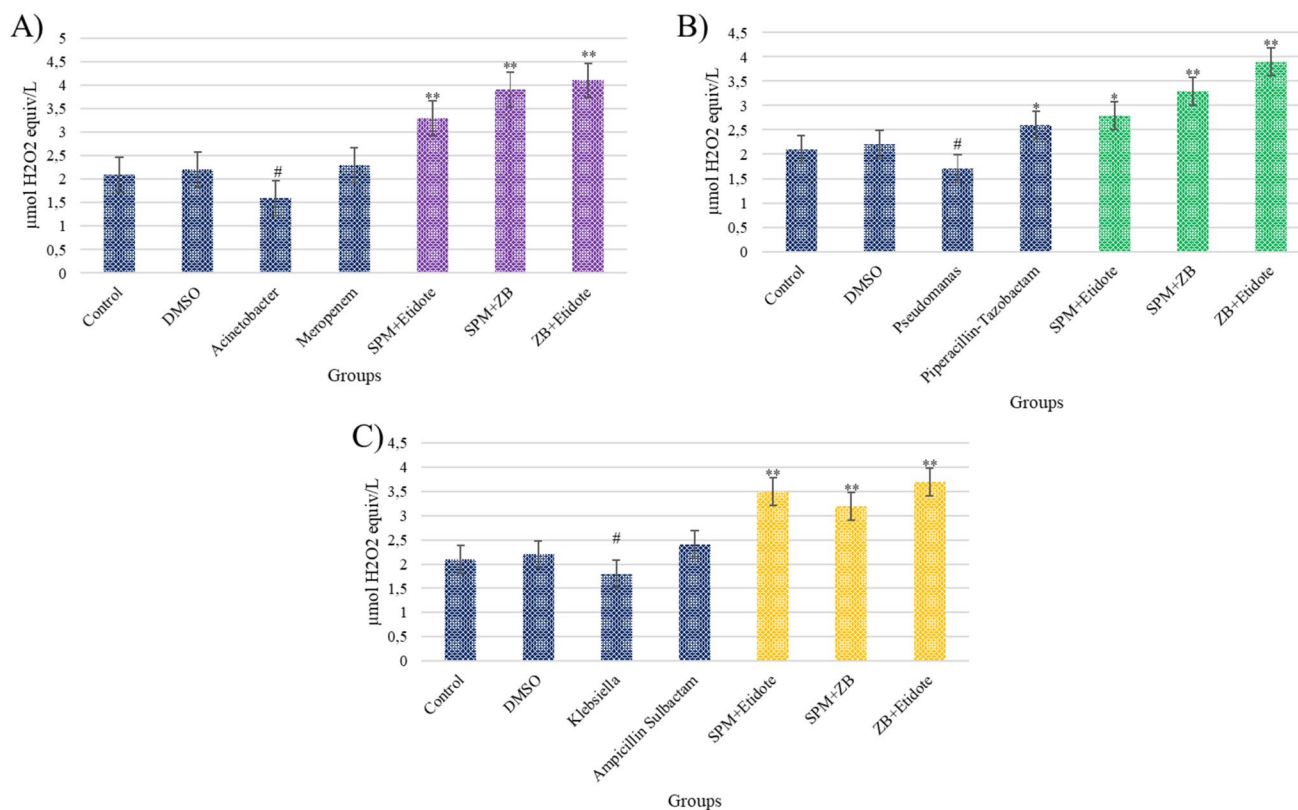


**Fig. 3** TOS (total oxidant capacity) assay test. TOS assay results for **A** *Acinetobacter*—A549, **B** *P. aeruginosa*—A549, and **C** *K. pneumoniae*—A549, in cell culture after 24 h. # $P < 0.05$  compared with the

control group. \* $P < 0.05$  and \*\* $P < 0.001$  compared with the bacteria control group

lung cancer cell culture (Fig. 1). The MTT results obtained from *Acinetobacter* show an increase in cell viability ( $P < 0.001$ ) (Fig. 1A). When compared to the control group, meropenem therapy showed a substantial difference ( $P < 0.001$ ). The treatment viability ratio was compared with the bacteria control group. Boron compounds decreased cell viability ratio dose ( $\mu\text{g/ml}$ ): Etidote (125) + SPM (62.5) (126%,  $P < 0.05$ ) < SPM (62.5) + ZB (31.25) (110,  $P < 0.001$ ) < ZB (31.25) + Etidote (125) (109%,  $P < 0.001$ ) compared with the bacteria control group.

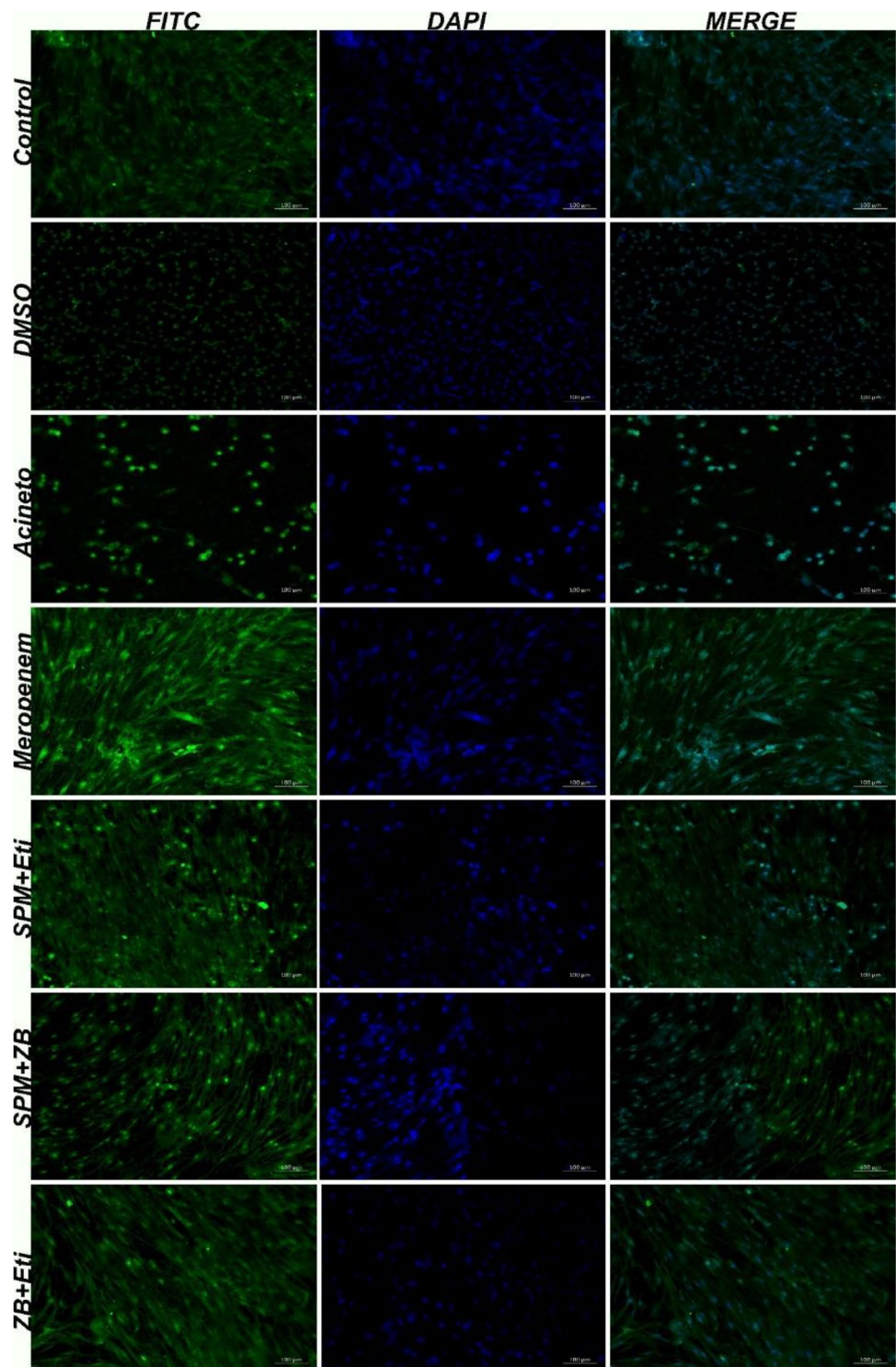
The MTT results obtained from *Pseudomonas aeruginosa* show an increase in cell viability by 164% ( $P < 0.001$ ) (Fig. 1B). A significant difference was found between the piperacillin-tazobactam treatment against the control group ( $P < 0.05$ ). The treatment viability ratio was compared with the bacteria control group. Boron compounds decrease cell viability ratio dose ( $\mu\text{g/ml}$ ): Etidote (125) + SPM (62.5) (128%,  $P < 0.05$ ) < SPM (62.5) + ZB (31.25) (124,  $P < 0.05$ ) < ZB (31.25) + Etidote (125) (112,  $P < 0.001$ ) compared with the bacteria control group.

The MTT results obtained from *Klebsiella pneumoniae* show an increase in cell viability ( $P < 0.001$ ) (Fig. 1A). A significant difference was found between

the ampicillin-sulbactam treatment against the control group ( $P < 0.001$ ). The treatment viability ratio was compared with the bacteria control group. Boron compounds decrease cell viability ratio dose ( $\mu\text{g/ml}$ ): SPM (62.5) + ZB (31.25) (129%,  $P < 0.05$ ) < Etidote (125) + SPM (62.5) (123%,  $P < 0.001$ ) < ZB (31.25) + Etidote (125) (119%,  $P < 0.001$ ) compared with the bacteria control group.

The boron compound effects on TAC levels of bacteria combined A549 lung cancer cell culture (Fig. 2). The TAC results obtained from (A) *Acinetobacter*—A549, (B) *Pseudomonas aeruginosa*—A549, and (C) *Klebsiella pneumoniae* show an increase in total antioxidant capacity ( $P < 0.05$ ). There was no discernible difference between the antibiotic treatment group (meropenem, piperacillin-tazobactam, and ampicillin-sulbactam) and the control group. The TAC status of the treatment groups was compared to the microbial control group. Boron compounds decrease TAC capacity in all groups. Compared to the *Acinetobacter* group, dose ( $\mu\text{g/ml}$ ), Etidote (125) + SPM (62.5) (4.7,  $P < 0.05$ ) < SPM (62.5) + ZB (31.25) (3.9,  $P < 0.001$ ) < ZB (31.25) + Etidote (125) (3.9,  $P < 0.001$ ) compared with the bacteria control group.

**Fig. 4** *A. baumannii*, expressions of 8-OHdG (FITC), IF, bar: 100  $\mu$ m in A549 lung cell line



Compared to the *Pseudomonas* group, dose ( $\mu$ g/ml), Etidote (125) + SPM (62.5) (4.6,  $P < 0.05$ ) < SPM (62.5) + ZB (31.25) (4.3,  $P < 0.05$ ) < ZB (31.25) + Etidote (125) (3.8,  $P < 0.001$ ) compared with the bacteria control group.

Compared to the *Klebsiella* group, dose ( $\mu$ g/ml), SPM (62.5) + ZB (31.25) (4.8,  $P < 0.05$ ) < Etidote (125) +

SPM (62.5) (4.6,  $P < 0.001$ ) < ZB (31.25) + Etidote (125) (4.3,  $P < 0.001$ ) compared with the bacteria control group.

The combined TOS levels of bacteria and A549 lung cancer cells are affected by the boron compound (Fig. 3). The total antioxidant capacity (TAC) values from (A) *Acinetobacter*—A549, (B) *P. aeruginosa*—A549, and (C) *K.*

**Table 6** *A. baumannii* analysis and statistical data of immunofluorescent results in cell culture

Groups	8-OHdG expression levels
Control	20.18 ± 0.42 <sup>a</sup>
DMSO	20.12 ± 0.16 <sup>a</sup>
<i>Acinetobacter</i>	81.32 ± 2.56 <sup>b</sup>
Meropenem	43.33 ± 1.26 <sup>c</sup>
SPM+Etidote	30.12 ± 1.49 <sup>d</sup>
SPM+ZB	29.84 ± 1.26 <sup>d</sup>
ZB+Etidote	29.49 ± 1.38 <sup>d</sup>

<sup>a,b,c,d</sup>Different letters on the same line represent statistically significant differences ( $p < 0.05$ )

*pneumoniae* indicate a decrease ( $P < 0.05$ ). Meropenem and ampicillin-sulbactam did not differ significantly from the control group when compared to the piperacillin-tazobactam ( $P > 0.05$ ), but there was a significant difference between the two. Treatment TOS status was compared with the bacteria control group. Boron compounds decrease TOS capacity in all groups. Compared to the *Acinetobacter* group, dose ( $\mu\text{g/ml}$ ), Etidote (125) + SPM (62.5) (3.3,  $P < 0.001$ ) < SPM (62.5) + ZB (31.25) (3.9,  $P < 0.001$ ) < ZB (31.25) + Etidote (125) (4.1,  $P < 0.001$ ) compared with the bacteria control group.

Compared to the *Pseudomonas* group, dose ( $\mu\text{g/ml}$ ), Etidote (125) + SPM (62.5) (2.8,  $P < 0.05$ ) < SPM (62.5) + ZB (31.25) (3.3,  $P < 0.001$ ) < ZB (31.25) + Etidote (125) (3.9,  $P < 0.001$ ) compared with the bacteria control group.

Compared to the *Klebsiella* group, dose ( $\mu\text{g/ml}$ ), SPM (62.5) + ZB (31.25) (3.7,  $P < 0.001$ ) < Etidote (125) + SPM (62.5) (3.5,  $P < 0.001$ ) < ZB (31.25) + Etidote (125) (3.2,  $P < 0.001$ ) compared with the bacteria control group.

## Immunofluorescence Results

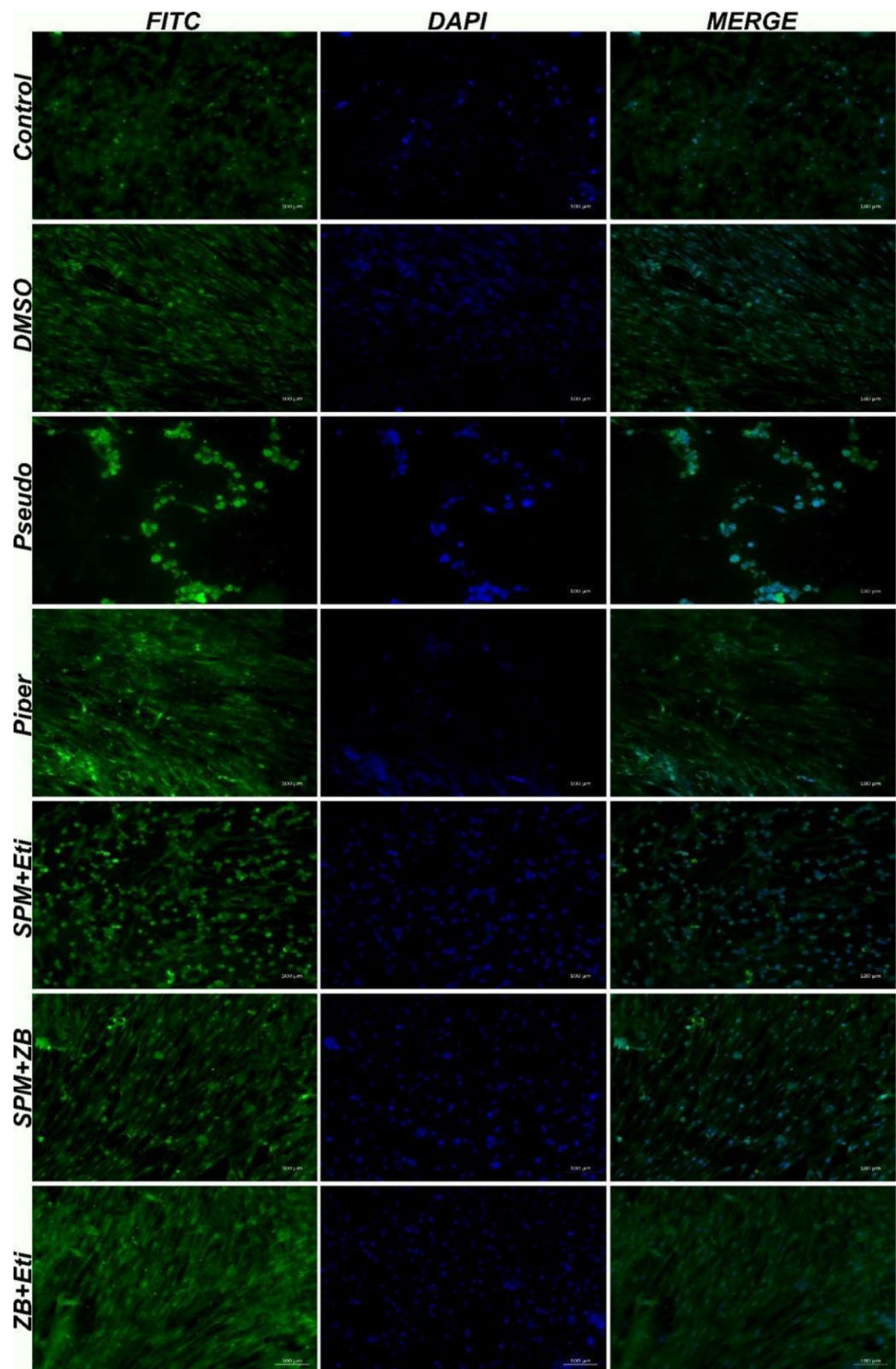
When *A. baumannii* was used as the control group, immunofluorescence labeling on the A549 lung cell line determined that 8-OHdG expressions were not present. Immunofluorescence labeling carried out in the A549 lung cell line resulted in an evaluation of the 8-OHdG expressions in the DMSO group as being negative. As a result of immunofluorescence staining performed on the A549 lung cell line, severe cytoplasmic 8-OHdG expressions were observed in the cells. Meropenem group immunofluorescence staining performed on the A549 lung cell line revealed moderate 8-OHdG expressions in the cell cytoplasm. In the SPM+Etidote group, as a result of immunofluorescence staining performed on the A549 lung cell line, mild intracytoplasmic 8-OHdG expressions were detected in the cell. When compared to

the *Acinetobacter* group, a statistically significant difference ( $P < 0.05$ ) was found. In the SPM+ZB group, as a result of immunofluorescence staining performed on the A549 lung cell line, mild 8-OHdG expressions were observed in the cells. When compared to the *Acinetobacter* group, a statistically significant difference ( $P < 0.05$ ) was found. In the ZB+Etidote group, as a result of immunofluorescence staining performed on the A549 lung cell line, mild cytoplasmic 8-OHdG expressions were detected in the cells. A statistically significant difference ( $P < 0.05$ ) was detected when compared with the *Acinetobacter* group (Fig. 4) (Table 6).

In *P. aeruginosa* of the control group, 8-OHdG expressions were evaluated as negative as a result of immunofluorescence staining performed in the A549 lung cell line. In the DMSO group, 8-OHdG expressions were evaluated as negative as a result of immunofluorescence staining performed in the A549 lung cell line. In the *Pseudomonas* group, as a result of immunofluorescence staining performed on the A549 lung cell line, severe cytoplasmic 8-OHdG expressions were detected in the cells. In the piperacillin-tazobactam group, immunofluorescence staining performed on the A549 lung cell line revealed moderate intracytoplasmic 8-OHdG expressions in the cells. In the SPM+Etidote group, as a result of immunofluorescence staining performed on the A549 lung cell line, mild intracytoplasmic 8-OHdG expressions were detected in the cells. When compared to the *Pseudomonas* group, a statistically significant difference ( $P < 0.05$ ) was found. In the SPM+ZB group, as a result of immunofluorescence staining performed on the A549 lung cell line, mild intracytoplasmic 8-OHdG expressions were observed in the cells. A statistically significant difference ( $P < 0.05$ ) was detected when compared with the *Pseudomonas* group. In the ZB+Etidote group, as a result of immunofluorescence staining performed on the A549 lung cell line, very mild 8-OHdG expressions were detected in cell cytoplasm. When compared to the *Pseudomonas* group, a statistically significant difference ( $P < 0.05$ ) was found (Fig. 5) (Table 7).

In *K. pneumoniae* of the control group, immunofluorescence labeling carried out in the A549 lung cell line was determined as negative for 8-OHdG expressions. Immunofluorescence labeling carried out in the A549 lung cell line resulted in an evaluation of the 8-OHdG expressions in the DMSO group as being negative. In the *Klebsiella* group, as a result of immunofluorescence staining performed on the A549 lung cell line, intense intracytoplasmic 8-OHdG expressions were detected in the cells. In the ampicillin-sulbactam group, immunofluorescence staining performed on the A549 lung cell line revealed moderate levels of 8-OHdG expressions in the cell cytoplasm. In the SPM+Etidote group, immunofluorescence staining performed on the A549 lung cell line revealed mild cytoplasmic 8-OHdG expressions in the cells. When

**Fig. 5** *P. aeruginosa*, expressions of 8-OHdG (FITC), IF, bar: 100  $\mu$ m in A549 lung cell line



compared to the *Klebsiella* group, a statistically significant difference ( $P < 0.05$ ) was found. In the SPM+ZB group, as a result of immunofluorescence staining performed on the A549 lung cell line, mild intracytoplasmic 8-OHdG expressions were observed in the cells. When compared to the *Klebsiella* group, a statistically significant difference

( $P < 0.05$ ) was found. In the ZB+Etidote group, as a result of immunofluorescence staining performed on the A549 lung cell line, mild 8-OHdG expressions were observed in the cell cytoplasm. When compared to the *Klebsiella* group, a statistically significant difference ( $P < 0.05$ ) was found (Fig. 6) (Table 8).

**Table 7** *P. aeruginosa* analysis and statistical data of immunofluorescent results in cell culture

Groups	8-OHdG expression levels
Control	18.26 ± 0.41 <sup>a</sup>
DMSO	18.12 ± 0.68 <sup>a</sup>
Pseudomonas	85.59 ± 2.84 <sup>b</sup>
Piperacillin-tazobactam	52.59 ± 1.49 <sup>c</sup>
SPM+Etidote	32.54 ± 1.98 <sup>d</sup>
SPM+ZB	30.3 ± 1.57 <sup>d</sup>
ZB+Etidote	25.89 ± 1 <sup>e</sup>

<sup>a,b,c,d,e</sup>Different letters on the same line represent statistically significant differences ( $p < 0.05$ )

### Presence of Carbapenemase Genes

Using specific primers for the OXA-48 and AIM genes, multiplex PCR was carried out to test for the presence of carbapenemase genes. In this study, the presence of the carbapenemase gene was analyzed before and after treatment (Fig. 7). Following the delivery of the drug, no AIM gene was found in the isolates that had both genes previously.

### Discussion

Among the nosocomial infectious agents, gram-negative bacteria, notably *A. baumannii*, *P. aeruginosa*, and *K. pneumoniae*, promote antibiotic resistance and cause problems in sepsis infections [25]. Especially thanks to the biofilm they developed, they had multidrug resistance [26].

Using nanoscale titania (nano-TiO<sub>2</sub>) and a double geometric isomer ferrocene-carborane derivative, Li et al. (2013) explored a novel method for preventing nosocomial infections brought on by multidrug-resistant bacteria like the *A. baumannii* strain. The remarkable improvement effect of TiO<sub>2</sub> nanoparticles on the antibacterial activity of FcSB1 or FcSB2 against clinically multidrug-resistant *A. baumannii* is shown by drug interaction assay and time-killing experiments. The FIC index values for the combination of FcSB1 and nano-TiO<sub>2</sub> are between 0.375 and 0.106 and for nano-TiO<sub>2</sub> and FcSB2 between 0.250 and 0.083, according to the relevant antibacterial activity (FIC index model) evaluated using a nonparametric technique. The antibacterial activity of FcSB1 or FcSB2 in combination with nano-TiO<sub>2</sub> on the target microorganisms is demonstrated [27].

In a study examining the effects of boron compounds (BGM and BGD), which were created as a new form of boron, on U87MG cells, it was found that U87MG GBM cells showed a cytotoxic effect and antibacterial effect against *S. aureus* and *E. coli* and were more beneficial than

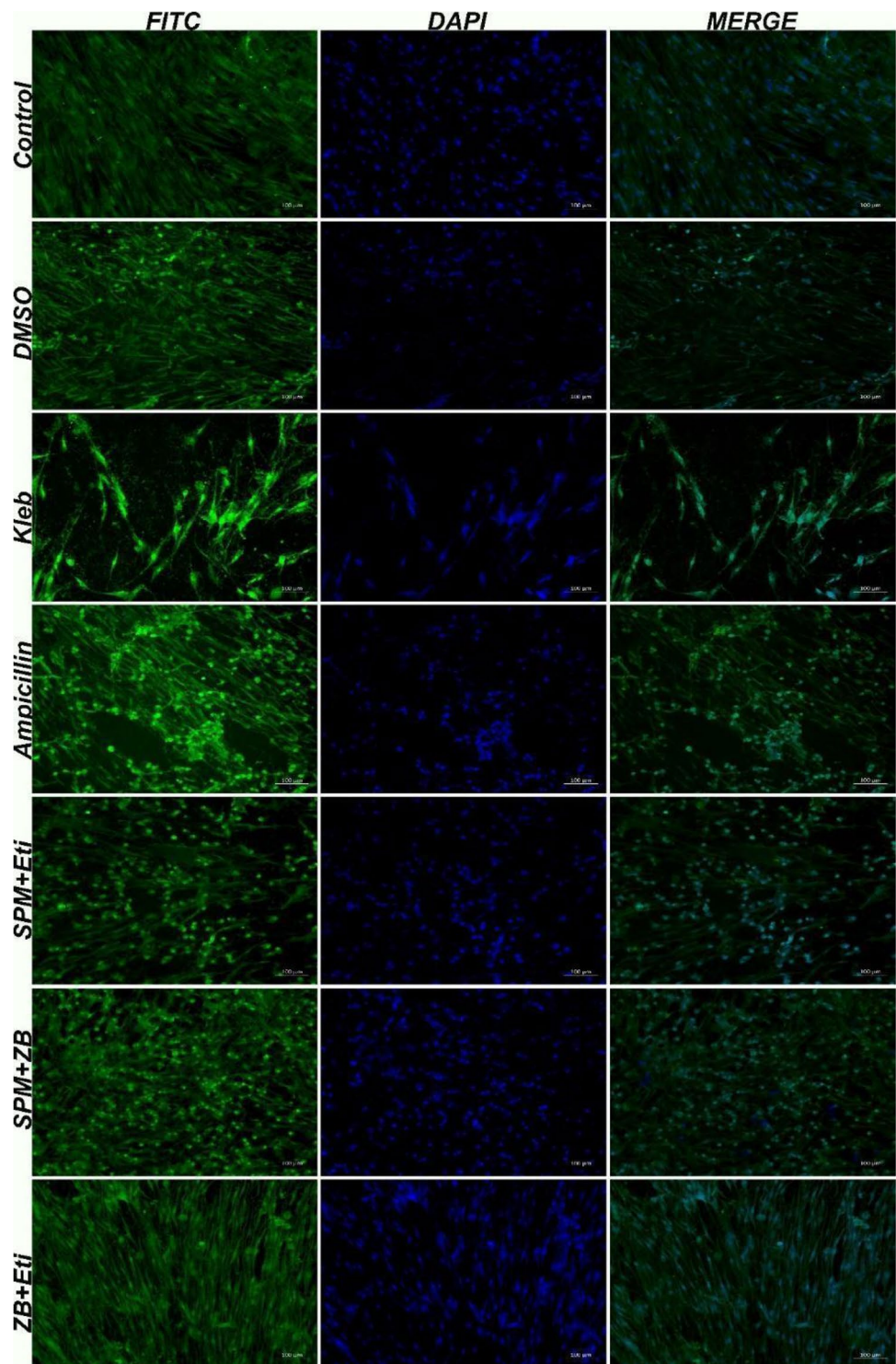
boron [28]. In their investigation on hepatocellular cancer, the same researchers claimed that the same boron synthesis chemicals exhibited cytotoxic, antioxidant, and antibacterial effects [29]. All of these details and the development of resistance profiles are closely related to a number of mechanisms, including biofilm formation and virulence elements, collectively referred to as the bacterial environment sensing system. Today, research into chemicals that prevent or interfere with these formations is required. Boron-derived compounds and studies looking at outcomes that are bactericidal, fungicidal, fungistatic, and antiviral have been published in the literature, in addition to the expanding amount of research on chemicals that can alter the bacterial verbal exchange system. According to a discovery, boric acid spinoff molecules can be employed to produce biofilms because of their antibacterial properties. Additionally, it has been hypothesized that boric acid molecules play a significant role in the development of *Vibrio harveyi*'s biofilm [29]. While the biofilm formation of *Enterococcus faecalis* was inhibited by boric acid [30], boron showed antimicrobial activity against *Candida albicans* [31] and many other pathogens [32–35].

It was discovered that AN3365, a novel boron-containing protein synthesis inhibitor, was effective against clinical isolates of Enterobacteriaceae and non-fermentative gram-negative bacteria, as well as a subset of strains of *Klebsiella pneumoniae* that produce the enzyme carbapenemase (KPC). It inhibited 92.2% of these. AN3365 was also less effective against multidrug-resistant *A. baumannii* and *Burkholderia cepacia*, but more effective against wild-type *A. baumannii* and *Stenotrophomonas maltophilia* [36].

According to Hu et al. (2021), *A. baumannii*'s minimum inhibitory concentration (MIC) for AgNPs made with *Artemisia argyi* leaf extract was 1 g/ml, and *S. aureus*, *Escherichia coli*, and *Candida albicans*' MICs were 2 g/ml. AgNPs against MBEC 50 strains of *Artemisia argyi* were produced with leaf extract, and their concentrations were found to be 2 g/ml for *A. baumannii*, 4 g/ml for *S. aureus*, 1/2 g/ml for *E. coli*, and 2 g/ml for *C. albicans*. Synthesized from *Artemisia argyi* leaf extract, the combination of AgNPs with clomiphene shows synergistic antibacterial and antibiofilm effects. FIC, or fractional inhibitory concentration, was found to be 0.5 [37].

In order to test the efficiency of boron compounds, we infected the A549 lung cancer cell line with *A. baumannii*, *K. pneumoniae*, and *P. aeruginosa*. To calculate the FIC index, antibiotic and boron compound concentrations created in accordance with MIC values were examined. Etidote+SPM 64 µg/ml + 1024 µg/ml on *A. baumannii*, 128 µg/ml + 512 µg/ml and (128 – 32) µg/ml + 32 µg/ml on *P. aeruginosa*, and 64 µg/ml + 32 µg/ml, 64 µg/ml + 512 µg/ml, 32 µg/ml + 64 µg/ml, and (64 – 32) µg/ml + 32 µg/ml doses on *K. pneumoniae* showed a synergistic effect.

**Fig. 6** *Klebsiella pneumoniae*, expressions of 8-OHdG (FITC), IF, bar: 100  $\mu$ m in A549 lung cell line



Etidote+ZB (64 – 32)  $\mu$ g/ml + 64  $\mu$ g/ml on *P. aeruginosa* and (64 – 32)  $\mu$ g/ml + 64  $\mu$ g/ml and (64 – 32)  $\mu$ g/ml + 32  $\mu$ g/ml on *K. pneumoniae* showed a synergistic effect. ZB+SPM showed a synergistic effect at doses of 32  $\mu$ g/ml + 32  $\mu$ g/ml on *P. aeruginosa* and (128 – 64) + 32  $\mu$ g/ml on *Klebsiella pneumoniae*. Antibiofilm activity was measured at 570 nm wavelength. In our study results, the antibiofilm

activity was determined respectively at the rate of 46.48%, 48.01%, and 44.34% in *A. baumannii* (ATCC19606)+boron compounds; 40.70%, 49.71%, and 48.03% in *P. aeruginosa* (ATCC 27853)+boron compounds; and 40.03%, 45.01%, and 44.44 in *K. pneumoniae* (ATCC700603).

Celebi et al. (2023) measured the minimum and fractional inhibitory concentration of boron compounds and

**Table 8** *K. pneumoniae* analysis and statistical data of immunofluorescent results in cell culture

Groups	8-OHdG expression levels
Control	22.54 ± 0.59 <sup>a</sup>
DMSO	24.03 ± 0.81 <sup>a</sup>
Klebsiella	92.58 ± 2.23 <sup>b</sup>
Ampicillin-sulbactam	59.49 ± 1.83 <sup>c</sup>
SPM+Etidote	39.43 ± 1.26 <sup>d</sup>
SPM+ZB	41.18 ± 1.84 <sup>d</sup>
ZB+Etidote	38.7 ± 1.67 <sup>d</sup>

<sup>a,b,c,d</sup>Different letters on the same line represent statistically significant differences ( $p < 0.05$ )

antibiofilm levels against *K. pneumoniae*. HepG2 cells were at the specified dosage levels. Immunofluorescent staining was carried out, shown, and assessed within the line's non-toxic dosage range. Boron compounds for sodium perborate monohydrate and antidote detect low and high minimum inhibitory concentration values, respectively. Monohydrate of sodium perborate was also discovered to be successful in biofilm production and resistance genes. The results demonstrate the combination of boron compounds. When employed as in the HepG2 cell line, it is more effective. The cytotoxic effect of boron compounds was discovered to be reduced due to its actions in the toxicity model [19].

In a study on the effects of boric acid derivatives on cytokine and redox stress parameters in a wound model infected with methicillin-resistant *Staphylococcus aureus*, potassium metaborate was found to be more effective and less toxic to fibroblast cells than boric acid. However, boric

acid and potassium metaborate have been discovered to display the potential to promote lesion resolution by considerably reducing the expression levels of inflammatory markers, even when IL-1 levels were high in the bacteria group [38].

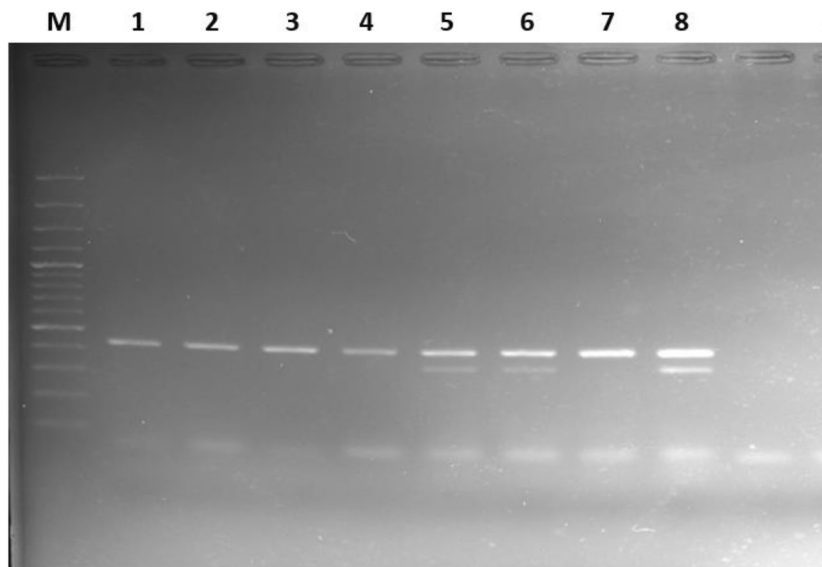
In a study using nine boron compounds, it was shown that in addition to having antibacterial and anticancer capabilities, they also had highly serious inhibitory activity against pathogens that build biofilms in a short amount of time (between 2 and 4 h), and they had an impact on resistance genes [39]. In a study conducted by Hernandez et al. to develop a new boron-based antibiotic, NDM-1 and KPC were found to be active against gram-negative bacteria such as carbapenemase-carrying *P. aeruginosa* and *E. coli* [40]. In a study with vaborbactam, a novel  $\beta$ -lactamase inhibitor based on boron ring structure, it was reported that vaborbactam showed antimicrobial activity due to its strong carbapenemase and  $\beta$ -lactamase inhibitory effects [41].

Alternative bacterial infection control methods stop the spread of pathogenic microorganisms. It may provide further therapy support. In this situation, boosting additional support studies is crucial for the therapy course [42, 43].

## Conclusion

The bioapplication of these boron derivatives in combination to fight nosocomial infection brought on by multidrug-resistant bacteria, such as *A. baumannii*, may be made clear by this work. Additional molecular analysis may help us understand the effects and workings of the chemicals we utilize. The limitation of the current study is the evaluation of interleukin-like IL-1, IL-6, and apoptosis markers

**Fig. 7** PCR sample images of lines 1–4 and 7; OXA-48 gene (438 bp). PCR sample images of lines 5, 6, and 8 AIM gene (322 bp). Before the drug was applied, the resistance gene images were represented by numbers 1–6, and after the substance was applied, the resistance gene images were represented by numbers 7–12



like caspase-3 and caspase-8 for the determination of cell response to bacterial contamination.

**Code Availability** Not applicable.

**Author Contribution** Concept—D.C., O.C., A.T., E.A., M.C.G., S.B., and S.Y. Design—D.C., O.C., E.A., A.T., S.B., and S.Y. Supervision—D.C., O.C., A.T., and S.Y. Resources—D.C., O.C., A.T., S.B., and S.Y. Materials—D.C., O.C., A.T., S.B., and S.Y. Data collection and/or processing—D.C., O.C., A.T., S.B., and S.Y. Analysis and/or Interpretation—D.C., O.C., A.T., S.B., and S.Y. Literature search—D.C., O.C., A.T., M.C.G., S.B., and S.Y. Writing—D.C., E.A., and S.Y. Critical reviews—D.C., O.C., A.T., M.C.G., and S.Y.

**Data Availability** Not applicable.

## Declarations

**Ethics Approval** Not applicable.

**Conflict of Interest** The authors declare no competing interests.

## References

- Vazquez-Lopez R, Rivero Rojas O, Ibarra Moreno A et al (2019) Antibiotic-resistant septicemia in pediatric oncology patients associated with post-therapeutic neutropenic fever. *Antibiotics (Basel)* 8:106
- Moghnieh R, Estaitieh N, Mugharbil A et al (2015) Third-generation cephalosporin-resistant Enterobacteriaceae and multidrug-resistant gram-negative bacteria causing bacteremia in febrile neutropenia adult cancer patients in Lebanon, broad-spectrum antibiotics use as a major risk factor, and correlation with poor prognosis. *Front Cell Infect Microbiol* 5:11
- Trecarichi EM, Tumbarello M (2014) Antimicrobial-resistant gram-negative bacteria in febrile neutropenic patients with cancer: current epidemiology and clinical impact. *Curr Opin Infect Dis* 27:200–210
- Dursun A, Özsoyul S, Kılıç H, Ulu Kılıç A, Akyıldız BN (2018) Antibiotic susceptibilities of *Pseudomonas aeruginosa*, *Klebsiella pneumoniae* and *Acinetobacter baumannii* strains isolated from patients in the pediatric intensive care unit. *Turk J Intensive Care* 16(3):109–114
- Papp-Wallace KM, Endimiani A, Taracila MA, Bonomo RA (2011) Carbapenems: past, present, and future. *Antimicrob Agents Chemother* 55:4943–4960
- El-Gamal MI, Brahim I, Hisham N, Aladdin R, Mohammed H, Bahaeldin A (2017) Recent updates of carbapenem antibiotics. *Eur J Med Chem* 131:185–195
- Frakking FNJ, Rottier WC, Dorigo-Zetsma W, van Hattem JMA, van Hees BC, Klutymans JAWJN et al (2013) Appropriateness of empirical treatment and outcome in bacteremia caused by extended-spectrum- $\beta$ -Lactamase-producing bacteria. *Antimicrob Agents Chemother* 57:3092–3099
- Codjoe FS, Donkor ES (2018) Carbapenem resistance: a review. *Med Sci* 6:e1
- Poole K (2011) *Pseudomonas aeruginosa*: resistance to the max. *Front Microbiol* 2:e65
- Hill KE, Malic S, McKee R, Rennison T, Harding KG, Williams DW et al (2010) An in vitro model of chronic wound biofilms to test wound dressings and assess antimicrobial susceptibilities. *J Antimicrob Chemother* 65(6):1195–1206
- Yarwood JM, Schlievert PM (2003) Quorum sensing in Staphylococcus infections. *J Clin Invest* 112(11):1620–1625
- Tran PL, Lowry N, Campbell T, Reid TW, Webster DR, Tobin E et al (2012) An organoselenium compound inhibits Staphylococcus aureus biofilms on hemodialysis catheters in vivo. *Antimicrob Agents Chemother* 56(2):972–978
- Scorei R (2012) Is boron a prebiotic element? A mini-review of the essentiality of boron for the appearance of life on earth. *Orig Life Evol Biosph* 42:3–17
- Ali F, Hosmane NS, Zhu Y (2020) Boron chemistry for medical applications. *Molecules* 25:828
- Tombuloglu A, Copoglu H, Aydin-Son Y, Guray NT (2020) In vitro effects of boric acid on human liver hepatoma cell line (HepG2) at the half-maximal inhibitory concentration. *J Trace Elem Med Biol* 62:126573
- Wei Y, Yuan FJ, Zhou WB, Wu L, Chen L, Wang JJ, Zhang YS (2016) Borax-induced apoptosis in HepG2 cells involves p53, Bcl-2, and Bax. *Genet Mol Res* 15(2). <https://doi.org/10.4238/gmr.15028300>
- Köse DA (2008) Preparation and structure investigation of biopotent boron compounds with hydroxy-functionalized organic molecules. Hacettepe University, Science Institute, Ankara
- Celebi D, Taghizadehghalehjouhi A, Baser S, Genc S, Yilmaz A, Yeni Y, Tsatsakis A (2022) Effects of boric acid and potassium metaborate on cytokine levels and redox stress parameters in a wound model infected with methicillin-resistant Staphylococcus aureus. *Mol Med Rep* 26(3):1–11
- Celebi O, Celebi D, Taghizadehghalehjouhi A, Baser S, Güler MC, Yıldırım S (2023). The antibacterial effect of boron compounds and evaluation of the effects on biofilm formation in the infection model of *Klebsiella pneumoniae* on the HepG2 cell line. *J Contemp Med* 13(1): 1–7
- Celebi D, Aydın E, Rakici E et al (2023) Evaluation of presence of clone ST131 and biofilm formation in ESBL producing and non-producing *Escherichia coli* strains. *Mol Biol Rep* 50:5949–5956. <https://doi.org/10.1007/s11033-023-08532-z>
- Ruzin A, Petersen PJ, Jones CH (2010) Resistance development profiling of piperacillin in combination with the novel beta-lactamase inhibitor BLI-489. *J Antimicrob Chemother* 65(2):252–257
- Haste NM, Hughes CC, Tran DN, Fenical W, Jensen PR, Nizet V (2011) Pharmacological properties of the marine natural product marinopyrrole A against methicillin-resistant Staphylococcus aureus. *Antimicrob Agents Chemother* 55(7):3305–3312
- Ausubel FM, Brient R, Kingston RE, Moore DD, Seidman JG, Smith JA et al (1995) Short protocols in molecular biology, 2nd edn. John Wiley & Sons, New York
- Poirel L, Walsh TR, Cuvillier V, Nordmann P (2011) Multiplex PCR for detection of acquired carbapenemase genes. *Diagn Microbiol Infect Dis* 70:119–123
- Peleg AY, Hooper DC (2010) Hospital-acquired infections due to gram-negative bacteria. *N Engl J Med* 362(19):1804–1813
- Cha JO, Yoo JI, Yoo JS, Chung HS, Park SH, Kim HS et al (2013) Investigation of biofilm formation and its association with the molecular and clinical characteristics of methicillin-resistant Staphylococcus aureus. *Osong Public Health Res Perspect* 4(5):225–232
- Li S, Wu C, Zhao X, Jiang H, Yan H, Wang X (2013) Synergistic antibacterial activity of new isomeric carborane derivatives through combination with nanoscaled titania. *J Biomed Nanotechnol* 9(3):393–402
- Koldemir-Gündüz M, Aydin HE, Berikten D, Kaymak G, Köse DA, Arslantaş A (2021) Synthesis of new boron derived compounds; anticancer, antioxidant and antimicrobial effect in vitro glioblastoma tumor model. *J Korean Neurosurg Soc*. Nov 64(6):864–872

29. Koldemir-Gündüz M, Bolat M, Kaymak G, Berikten D, Köse DA (2022) Therapeutic effects of newly synthesized boron compounds (BGM and BGD) on hepatocellular carcinoma. *Biol Trace Elem Res* 200(1):134–146
30. Ni N, Li M, Wang J, Wang B (2009) Inhibitors and antagonists of bacterial quorum sensing. *Med Res Rev* 29(1):65–124
31. Zan R, Hubbezoglu I, Sumer Z, Tunc T, Tanalp J (2013) Antibacterial effects of two different types of laser and aqueous ozone against *Enterococcus faecalis* in root canals. *Photomed Laser Surg* 31(4):150–154
32. Pointer BR, Boyer MP, Schmidt M (2015) Boric acid destabilizes the hyphal cytoskeleton and inhibits invasive growth of *Candida albicans*. *Yeast* 32(4):389–398
33. Ahmad S, Haque MM, Ashraf SM, Ahmad S (2004) Urethane modified boron filled polyesteramide: a novel anti-microbial polymer from a sustainable resource. *Eur Polym J* 40:2097–2104
34. Yılmaz MT (2012) Minimum inhibitory and minimum bactericidal concentrations of boron compounds against several bacterial strains. *Turk J Med Sci* 42(2):1423–1429
35. Sarac N, Ugur A, Boran R, Elgin ES (2015) The use of boron compounds for stabilization of lipase from *Pseudomonas aeruginosa* ES3 for the detergent industry. *J Surfactant Deterg* 18(2):275–285
36. Sayin Z, Ucan US, Sakmanoglu A (2016) Antibacterial and antibiofilm effects of boron on different bacteria. *Biol Trace Elem Res* 173:241–246
37. Mendes RE, Alley MR, Sader HS, Biedenbach DJ, Jones RN (2013) Potency and spectrum of activity of AN3365, a novel boron-containing protein synthesis inhibitor, tested against clinical isolates of Enterobacteriaceae and non fermentative gram-negative bacilli. *Antimicrob Agents Chemother* 57(6):2849–2857
38. Hu L, Yang X, Yin J, Rong X, Huang X, Yu P, He Z, Liu Y (2021) Combination of AgNPs and domiphen is antimicrobial against biofilms of common pathogens. *Int J Nanomedicine* 16:7181–7194
39. Celebi O, Celebi D, Baser S, Aydın E, Rakıcı E, Uğraş S, Ağyar Yoldaş P, Baygutalp NK, & El-Aty AMA (2023) Antibacterial activity of boron compounds against biofilm-forming pathogens. *Biol Trace Elem Res*. <https://doi.org/10.1007/s12011-023-03768-z>
40. Hernandez V, Crépin T, Palencia A, Cusack S, Akama T, Baker SJ, Plattner JJ (2013) Discovery of a novel class of boron-based antibacterials with activity against gram-negative bacteria. *Antimicrob Agents Chemother* 57(3):1394–1403
41. Bhowmick T, Weinstein MP (2020) Microbiology of meropenem-vaborbactam: a novel carbapenem beta-lactamase inhibitor combination for carbapenem-resistant Enterobacterales infections. *Infect Dis Ther* 9:757–767
42. Celebi O, Taghizadehghalehjoughi A, Celebi D, Mesnage R, Golokhvast KS, Arsene AL, Tsatsakis A (2023) Effect of the combination of *Lactobacillus acidophilus* (probiotic) with vitamin K3 and vitamin E on *Escherichia coli* and *Staphylococcus aureus*: an in vitro pathogen model. *Mol Med Rep* 27(6):1–12
43. Celebi D, Celebi O, Baser S, Taghizadehghalehjoughi A (2023) Evaluation of Antimicrobial and Antibiofilm Efficacy of Bee Venom and Exosome Against *Escherichia coli* K99 Strain. *Kafkas Univ. Vet. Fak. Derg* 29(3):239–246. <https://doi.org/10.9775/kvfd.2023.29132>

**Publisher's Note** Springer Nature remains neutral with regard to jurisdictional claims in published maps and institutional affiliations.

Springer Nature or its licensor (e.g. a society or other partner) holds exclusive rights to this article under a publishing agreement with the author(s) or other rightsholder(s); author self-archiving of the accepted manuscript version of this article is solely governed by the terms of such publishing agreement and applicable law.